

1,2-Ferrocenediylazaphosphinines: An Unusual Coordination Behavior and Application to Allylic Alkylation

Thanh Thien Co, Seung Whan Paek, Sang Chul Shim, Chan Sik Cho, and
Tae-Jeong Kim*

Department of Industrial Chemistry, Kyungpook National University, Taegu, Korea 702-701

Dong Woong Choi and Sang Ook Kang

Department of Chemistry, Korea University, 208 Seochang, Chochiwon,
Chung-nam, Korea 339-700

Jong Hwa Jeong

Department of Chemistry, Kyungpook National University, Taegu, Korea 701-702

Received November 7, 2002

The reaction of 1,2-ferrocenediylazaphosphinines (**1a**, $R^1 = H$; **1b**, $R^1 = Me$; **1c**, $R^1 = Ph$) with $M(CO)_6$ ($M = Mo, W$), $MX(CO)_5$ ($M = Mn, Re$; $X = Br, Cl$), and $[Pd(\eta^3-C_3H_5)Cl]_2$ shows a strong tendency to adopt an unusual chelating bidentate coordination through nitrogen and the carbonyl oxygen, yielding $M(\eta^2-N,O)(CO)_4$ (**2**, $M = Mo$; **3**, $M = W$), $M(\eta^2-N,O)(X)(CO)_3$ (**6**, $M = Mn$, $X = Br$; **7**, $M = Re$, $X = Cl$), and $[Pd(\eta^2-N,O)(\eta^3-C_3H_5)]BF_4$ (after treatment with $AgBF_4$) (**8**), respectively. X-ray crystallographic structure determinations of **3a** ($R^1 = H$) and **8a** ($R^1 = H$) show the formation of a five-membered metallacycle with the distance of the metal–carbonyl oxygen bond being shorter than that of the metal–nitrogen bond in both compounds. The complexes **2** and **3** further undergo oxidative addition with allyl iodide to yield the corresponding $M(II)$ complexes of the type $[M(\eta^2-N,O)(\eta^3-C_3H_5)(I)(CO)_2]$ (**4**, $M = Mo$; **5**, $M = W$). Complexes **2–5** and **8** were employed as catalysts for nucleophilic allylic substitution of allyl acetates as a probe for both regio- and enantioselectivities of the reaction. All reactions involving unsymmetrical allyl acetates (E)- $RCH=CHCH_2OAc$ ($R = Pr, Ph$) led exclusively to the formation of achiral linear product (E)- $RCH=CHCH_2Nu$ regardless of the type of catalysts, the ligand, or the allyl substrate employed. One exception to the above statement is the observation that Mo- and W-based catalysts (**2–5**) are totally inactive toward the allylic substitution of cinnamyl acetate ($R = Ph$). Asymmetric allylic alkylation of a symmetrically 1,3-disubstituted substrate, $PhCH=CHCH(OAc)Ph$, is accomplished only by Pd-catalysts (**8**) with enantiomeric excesses up to 50% ee.

Introduction

We have recently shown that the reaction of 1-(α -aminoalkyl)-2-diphenylphosphinoferrocene with glyoxals results in, via an unusual cyclization, 1,2-ferrocenediylazaphosphinines (**1a–c**, Scheme 1) rather than the expected condensation product of bisferrocenyldiimines.¹ These compounds constitute a completely new family of planar chiral ferrocenes that are of intense current research interest in the field of asymmetric catalysis.^{2,3} We have further demonstrated that our new compounds

(**1a–c**) are not only powerful ligands in a Cu-catalyzed cyclopropanation of styrene to achieve a complete diastereoselectivity^{1,4} but also nucleophilic catalysts for highly regio- and enantioselective ring opening of epoxides.⁵ Intrigued by these observations and motivated by our continuing effort in the design and application of new ferrocene derivatives for use in asymmetric catalysis,⁶ we have extended our investigation with **1** to their reaction and coordination chemistry with various transition metal compounds that may find even wider application as catalysts in this area.

(1) Hwang, G.-H.; Ryu, E.-S.; Park, D.-K.; Shim, S. C.; Cho, C. S.; Kim, T.-J.; Jeong, J. H.; Cheong, M. *Organometallics* **2001**, *20*, 5784.

(2) For recent reviews on the synthesis and the use of planar chiral ferrocenes in asymmetric catalysis, see: (a) Richards, C. J.; Locke, A. J. *Tetrahedron: Asymmetry* **1998**, *9*, 2377. (b) Kagan, H. B.; Riant, O. In *Advances in Asymmetric Synthesis*; Hassner, A., Ed.; JAI Press Inc.: Greenwich, CT, 1997; Vol. 2, p 189. (c) Togni, A. In *Ferrocenes: Homogeneous Catalysis, Organic Synthesis, Materials Science*; Togni, A., Hayashi, T., Eds.; VCH: Weinheim, Germany, 1995; Chapters 2–4.

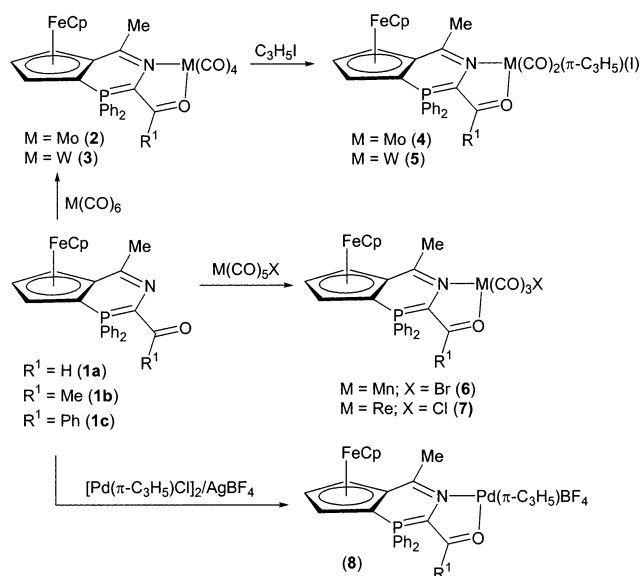
(3) For recent reviews on heterocyclic analogues of planar chiral ferrocenes such as aza- and phosphoferrocenes, see: (a) Ganter, C. J. *Chem. Soc., Dalton Trans.* **2001**, 3541. (b) Fu, G. C. *Acc. Chem. Res.* **2000**, *33*, 412, and references therein.

(4) Paek, S. H.; Co, T.-T.; Lee, D. H.; Park, Y. C.; Kim, T.-J. *Bull. Korean Chem. Soc.* **2002**, *23*, 1702.

(5) Unpublished results in this laboratory.

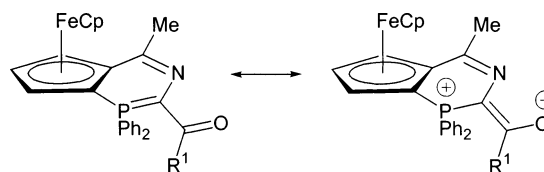
(6) (a) Song, J.-H.; Cho, D.-J.; Jeon, S.-J.; Kim, Y.-H.; Kim, T.-J. *Inorg. Chem.* **1999**, *38*, 893. (b) Cho, D.-J.; Jeon, S.-J.; Kim, H.-S.; Cho, C. S.; Shim, S. C.; Kim, T.-J. *Tetrahedron: Asymmetry* **1999**, *10*, 3833. (c) Cho, D.-J.; Jeon, S.-J.; Kim, H.-S.; Kim, T.-J. *Synlett* **1998**, 617. (e) Kim, T.-J.; Lee, H.-Y.; Ryu, E.-S.; Park, D.-K.; Cho, C. S.; Shim, S. C.; Jeong, J. H. *J. Organomet. Chem.* **2002**, *649*, 258. (f) Park, D.-K.; Ryu, E.-S.; Paek, S. H.; Shim, S. C.; Cho, C. S.; Kim, T.-J. *Bull. Korean Chem. Soc.* **2002**, *23*, 721.

Scheme 1



Our initial finding is an unusual chelating bidentate mode of **1** through nitrogen and carbonyl oxygen, an η^2 -N,O chelation, toward a range of transition metals such as $M(\text{CO})_6$ ($M = \text{Mo}, \text{W}$), $\text{MX}(\text{CO})_5$ ($M = \text{Mn}, \text{Re}$; $X = \text{Cl}, \text{Br}$), and $[\text{Pd}(\eta^3\text{-C}_3\text{H}_5)\text{Cl}]_2$, leading to the formation of $M(\eta^2\text{-N,O})(\text{CO})_4$, $[M(\eta^2\text{-N,O})(\eta^3\text{-C}_3\text{H}_5)(\text{I})(\text{CO})_2]$ (after oxidative addition of $\text{C}_3\text{H}_5\text{I}$), $M(\eta^2\text{-N,O})(X)(\text{CO})_3$, and $[\text{Pd}(\eta^2\text{-N,O})(\eta^3\text{-C}_3\text{H}_5)]\text{BF}_4$ (after treatment with AgBF_4), respectively. The attractiveness of these compounds derives from their potential attributes of chemo-, regio-, or stereoselectivity in catalytic allylic alkylation of various allylic acetates. For instance, unsymmetrically 1,3-disubstituted allyl derivatives such as $\text{RCH}=\text{CHCH}_2\text{-OAc}$ ($\text{R} = \text{Pr}, \text{Ph}$) are particularly demanding substrates, because, in addition to the requirement of enantiocontrol, the problem of regioselectivity has to be resolved.⁷ With most palladium catalysts, such substrates react with soft carbon nucleophiles preferentially at the less substituted terminus, giving rise to an achiral linear product.⁸ With certain molybdenum and tungsten catalysts incorporating phosphinodihydrooxazoles or bis(pyridine), on the other hand, such propensity is generally reversed to yield chiral, branched regioisomers.⁹ However, our own investigation on the same reaction by employing **2–5** and **8** as catalyst argues against the rule of thumb stated above, demonstrating that near perfect regioselectivity in favor of a linear

Scheme 2



isomer is attained regardless of the reaction parameters such as metal, ligand, or allyl substrate employed. In contrast, all complexes but **8** in their enantiomerically pure forms show total inactivity toward asymmetric allylic alkylation of a symmetrically 1,3-disubstituted substrate, 1,3-diphenyl-2-propenyl acetate. These observations along with the reaction and coordination chemistry of **1** with a series of transition metal complexes will be presented in this paper.

Results and Discussion

Synthesis. Scheme 1 demonstrates that all reactions lead to η^2 -N,O chelation, forming a five-membered metallacyclic ring as confirmed by various spectroscopic, analytical, and X-ray crystallographic techniques. These observations are rather unusual considering the fact that a simple carbonyl oxygen is a poor ligand for an organometallic fragment, although it is quite common for an amide carbonyl to be involved in coordination as a hemilabile chelating η^2 -N,O or η^2 -P,O ligand (vide infra). Thus, to the best of our knowledge, they constitute the first isolated and fully characterized representative of the complexes where a simple ketonic (or aldehydic) oxygen participates in chelation. It is tempting to propose that the extended resonance leading to an enolate such as shown in Scheme 2, in addition to the chelate effect, may partially be responsible for such a unique coordination behavior. For comparison, it is worth noting that a structurally related mode of η^2 -N,O or η^2 -P,O chelation involving a carbonyl oxygen can be found with some donors incorporating a carboxylic amide group. Recent examples for the former case include (1) a neutral bimetallic Mo(I) complex, $\{\text{MoCl}(\eta^3\text{-C}_3\text{H}_5)(\text{CO})_2\}_2\text{-}\mu\text{-trans-1,2-bis(2-pyridinecarboxamide)-cyclohexane}$, where the bridge bis(chelate) ligand involves coordination of an amide carbonyl oxygen and a pyridine nitrogen,¹⁰ and (2) a neutral Mo(0) complex, $\text{Mo}(\text{CO})_3[\eta^3\text{-1,2-bis(dihydrooxazolocarbonyl)-cyclohexane}]$, where the ligand binds to Mo with the two dihydrooxazole rings and one of the amide carbonyl oxygens.^{9e} The examples for the latter case are ubiquitous and can be found mostly in connection with Pd-complexes.¹¹ These include (1) a cationic Pd(II) complex of an acetamide-derived η^2 -P,O ligand, $[\text{PdMe}\{\eta^2\text{-PPh}_2\text{-NHC(O)Me}\}\{\text{PPh}_2\text{NHC(O)Me}\}]$,^{11d} and (2) a cationic bimetallic Pd(II) complex incorporating the Trost ligand, $[\text{Pd}(\eta^3\text{-C}_3\text{H}_5)]_2\text{-}\mu\text{-trans-1,2-diaminocyclohexane-}N,N'$

(7) For comprehensive recent reviews on the issue of regioselectivity of unsymmetrically substituted 1,3-allyl derivatives, see: (a) Trost, B. M.; Lee, C. In *Catalytic Asymmetric Synthesis*; Ojima, I., Ed.; Wiley-VCH: New York, NY, 2000; pp 593–650. (b) Pfaltz, A.; Lautens, M. In *Comprehensive Asymmetric Catalysis*; Jacobsen, E. N., Pfaltz, A., Yamamoto, H., Eds.; Springer: Berlin, Germany, 1999; Vol. II, pp 833–884.

(8) Godleski, S. A. In *Comprehensive Organic Synthesis*; Trost, B. M., Fleming, I., Semmelhack, M. F., Eds.; Pergamon Press: Oxford, U.K., 1991; Vol. 4, pp 585–662. (b) However, for recent interesting exceptions with Pd catalysis, see: Hayashi, T.; Kawatsura, M.; Uozumi, Y. *Chem. Commun.* **1997**, 561. Prétôt, R.; Pfaltz, A. *Angew. Chem., Int. Ed.* **1998**, 37, 323.

(9) (a) Lloyd-Jones, G. C.; Pfaltz, A. *Angew. Chem., Int. Ed. Engl.* **1995**, 34, 462. (b) Trost, A. M.; Hachiya, I. *J. Am. Chem. Soc.* **1998**, 120, 1104. (c) Glorius, F.; Pfaltz, A. *Org. Lett.* **1999**, 1, 142. (d) Belda, O.; Kaiser, N.-F.; Bremberg, U.; Larhed, M.; Hallberg, A.; Moberg, C. *J. Org. Chem.* **2000**, 65, 5868. (e) Glorius, F.; Neuburger, M.; Pfaltz, A. *Helv. Chim. Acta* **2001**, 84, 3178. (f) Trost, M.; Dogra, K.; Hayachi, I.; Emura, T.; Hughes, D. L.; Kraska, S.; Reamer, R. A.; Palucki, M.; Yasuda, N.; Reider, P. J. *Angew. Chem., Int. Ed.* **2002**, 41, 1929.

(10) Morales, D.; Pérez, J.; Riera, L.; Corzo-Suárez, R.; García-Granda, S.; Miguel, D. *Organometallics* **2002**, 21, 1540.

(11) For some examples of X-ray crystallographically characterized complexes of this type, see: (a) Braunstein, P.; Douce, L.; Fischer, J.; Graig, N. C.; Goetz-Grandmont, G.; Matt, D. *Inorg. Chim. Acta* **1992**, 194, 151. (b) Andrieu, J.; Braunstein, P.; Drillon, M.; Ingold, F.; Rabu, P.; Tiripicchio, A.; Uguzzoli, F. *Inorg. Chem.* **1996**, 35, 5986. (c) Leung, P. H.; Loh, S. K.; Vittal, J. J.; White, A. J. P.; Williams, D. J. *Chem. Commun.* **1997**, 1987. (d) Braunstein, P.; Frison, C.; Morise, X.; Adams, R. D. *J. Chem. Soc., Dalton Trans.* **2000**, 2205.

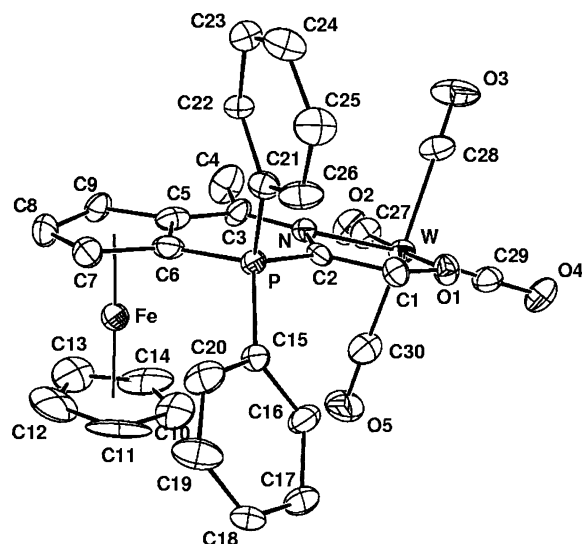


Figure 1. Crystal structure of **3a**. Thermal ellipsoids are drawn at 50% probability.

bis(2'-diphenylphosphinobenzoyl), where the bridge bis-(chelate) ligand involves coordination of an amide carbonyl oxygen and a phosphine to each metal.¹²

The syntheses of our new compounds (**2–8**) are quite straightforward. Gentle reflux of an equimolar mixture of **1** and $M(\text{CO})_6$ ($M = \text{Mo}, \text{W}$) in THF/toluene afforded **2** ($M = \text{Mo}$) and **3** ($M = \text{W}$) as dark red crystals after purification by column chromatography on silica gel.¹³ Analytical, spectroscopic, and X-ray crystal structure data in the case of **3a** are all consistent with their formulations. For example, three strong $\nu(\text{CO})$ bands from **2a** and **3a** are indicative of (*cis*-chelate) $M(\text{CO})_4$ (1882, 1855, 1803 cm^{-1} for **2a**; 1868, 1845, 1800 cm^{-1} for **3a**). Yet, due to the C_1 -symmetric nature of the ligand (**1**), all four carbonyls become nonequivalent in the given structure and thus give rise to four singlets in their ^{13}C NMR spectra (205.6, 206.2, 224.3, 225.2 ppm for **2a**; 204.0, 204.5, 216.5, 217.3 ppm for **3a**). An additional NMR spectral feature to be noted is a significant coordination shift ($\Delta\delta \approx 10$ ppm) found for the ylidic phosphorus signal, although this atom is not directly involved in the coordination with metal. A detailed NMR assignment for the complexes was made by comparison and by analogy with the NMR data for the ligand itself.¹⁴ A more conclusive structural confirmation comes from the X-ray crystal structure of **3a** shown in Figure 1. A summary of crystallographic data and selected bond lengths and angles are listed in Tables 1 and 2, respectively. The structure shows the geometry around tungsten to be a slightly distorted octahedron with *cis*-chelation of nitrogen and oxygen. Near perfect coplanarity encompassing the fused heteroaromatic ring of the ligand is further extended, on complexation, to the W-containing metallacyclic ring. The four W–CO bonds are of similar length and fall in the range 1.91(2)–2.04(2) Å. The W–O bond (2.19(1) Å)

Table 1. Summary of Crystallographic Data for **3a** and **8a**

	3a	8a
empirical formula	$\text{C}_{30}\text{H}_{22}\text{FeNO}_5\text{PW}$	$\text{C}_{29}\text{H}_{27}\text{BF}_4\text{FeNOPPd}$
fw	747.16	685.55
cryst size (mm)	$0.35 \times 0.40 \times 0.40$	$0.40 \times 0.40 \times 0.45$
space group	$P2_12_12_1$	$Pna2_1$
<i>a</i> (Å)	11.3160(8)	14.4365(12)
<i>b</i> (Å)	13.8693(10)	11.2483(6)
<i>c</i> (Å)	19.9330(16)	16.9363(11)
<i>V</i> (Å ³)	3128.4(4)	2750.2(3)
<i>Z</i>	4	4
<i>T</i> (K)	293(2)	293(2)
radiation, λ (Å)	Mo K α 0.71070	Mo K α 0.71070
θ range (deg)	1.79–25.97	2.17–25.47
data collected: <i>h</i> ; <i>k</i> ; <i>l</i>	0, 13; 0, 17; 0, 24	0, 17; –13, 0; 0, 20
no. of unique reflns	3431	2785
μ (mm ^{–1})	4.225	1.291
<i>F</i> (000)	1456	1376
refinement	FMLS on <i>F</i> ²	FMLS on <i>F</i> ²
GOF	1.222	1.069
<i>R</i> indices (<i>I</i> > 2 σ (<i>I</i>)) ^a	$R_1 = 0.0594$; $wR_2 = 0.1675$	$R_1 = 0.0494$; $wR_2 = 0.1346$
largest diff peak and hole (e/Å ³)	2.361 and –1.754	0.822 and –0.479

$$^a R_1 = \sum ||F_o| - |F_c|| / \sum |F_o|. \quad wR_2 = [\sum w(F_o^2 - F_c^2) / \sum w(F_o^2)]^{1/2}.$$

Table 2. Selected Bond Lengths (Å) and Angles (deg) for **3a** and **8a**

3a					
W–C(29)	1.91(3)	W–C(27)	1.94(2)	W–C(30)	1.98(3)
W–C(28)	2.04(2)	W–O(1)	2.19(1)	W–N	2.32(2)
C(1)–O(1)	1.28(2)	C(1)–C(2)	1.39(3)	N–C(2)	1.38(2)
N–C(3)	1.32(3)	P–C(2)	1.77(2)	P–C(6)	1.72(2)
C(3)–C(5)	1.41(3)	C(5)–C(6)	1.47(3)		
C(28)–W–C(30)	169(1)	C(29)–W–C(27)	88(1)		
C(27)–W–C(28)	85(1)	C(28)–W–C(29)	88.1(9)		
C(27)–W–O(1)	177.7(8)	N–W–C(29)	166.9(8)		
N–W–O(1)	74.0(5)	C(15)–P–C(21)	106.3(9)		
W–O(1)–C(1)	115(1)	C(2)–N–W	110(1)		
8a					
Pd–O	2.082(9)	Pd–N	2.137(8)	P–C(6)	1.762(5)
P–C(2)	1.774(8)	P–C(15)	1.792(6)	P–C(21)	1.804(5)
N–C(3)	1.28(1)	N–C(2)	1.43(1)	O–C(1)	1.30(1)
C(1)–C(2)	1.35(2)	C(3)–C(5)	1.47(1)	C(3)–C(4)	1.51(1)
O–Pd–N	81.8(3)	C(6)–P–C(2)	102.6(4)		
C(3)–N–C(2)	122.9(8)	C(3)–N–Pd	131.1(7)		
C(2)–N–Pd	105.9(6)	C(1)–O–Pd	109.3(7)		
O–C(1)–C(2)	124.2(9)	C(1)–C(2)–N	118.4(8)		
N–C(2)–P	124.5(7)	N–C(3)–C(5)	125.2(8)		

is shorter than the W–N bond (2.32(2) Å). Parallel observations are found with $\text{Mo}(\text{CO})_3[\eta^3\text{-1,2-bis(dihydrooxazolecarboxamide)cyclohexane}]$, where the bond distances of Mo–O and Mo–N are 2.2685(5) and 2.347(5) Å, respectively.^{9e} The C(1)–C(2) distance (1.39(2) Å) carries a partial multiple-bond character, supporting our proposal concerning the resonance structure in Scheme 2. Numerical parameters for the ligand remain almost the same upon complexation.

The complexes **2** and **3** readily undergo oxidative addition by allyl iodide to give the corresponding M(II) complexes $[\text{M}(\eta^2\text{-N,O})(\eta^3\text{-C}_3\text{H}_5)(\text{I})(\text{CO})_2]$ (**4**, $M = \text{Mo}$; **5**, $M = \text{W}$), respectively.^{15,16} Their synthesis may be justified in that they may not only serve as catalyst precursors for the allylic alkylation but also exist as

(12) Butts, C. P.; Crosby, J.; Lloyd-Jones, G. C.; Stephen, S. C. *Chem. Commun.* **1999**, 1707.

(13) For an unknown reason, the reaction of $\text{Cr}(\text{CO})_6$ with **1** did not lead to the formation of the expected product ($\eta^2\text{-N,O})\text{Cr}(\text{CO})_4$ even under harsh reaction conditions during an extended period of time.

(14) Complete NMR data for **1** are provided in the Supporting Information, ref 1.

(15) Dieck, H. T.; Friedel, H. J. *Organomet. Chem.* **1968**, *14*, 375.

(16) Hull, C. G.; Stiddard, M. H. B. *J. Organomet. Chem.* **1967**, *9*, 519.

reactive intermediates in the catalytic cycle as a result of oxidative addition to an electron-rich zerovalent species. Subsequent alkylation either directly to the allyl or to the metal followed by an alkyl-to-allyl migration with concomitant reductive elimination of the resulting olefin would complete the cycle.^{7,17} With soft nucleophiles $[M(L-L)(\eta^3-C_3H_5)(X)(CO)_2]$ ($L-L$ = bipy, phen; X = halide) complexes are known to react to afford olefins.¹⁸ Yet with hard nucleophiles such as alkyl and acetylide anions alkylation takes place selectively at the metal, and neither acyl complexes nor allylic alkylation products are formed.¹⁹

The structural identifications for **4** and **5** were performed without difficulty. Thus, for example, the persistence of a *cis*- $M(CO)_2$ unit is confirmed by infrared and ^{13}C NMR spectra showing, respectively, two strong $\nu(CO)$ bands (1923 and 1831 cm^{-1} for **4a**; 1912 and 1814 cm^{-1} for **5a**) and two carbonyl singlets (227.4 and 227.9 for **4a**). In addition, the pattern of three multiplets arising from *anti*- and *syn*-protons (H_{29}/H_{31}) and the central proton (H_{30}) in 1H NMR is diagnostic of a static (without fast equilibrium to η^1) $\eta^3-C_3H_5$ group like the one present in related $[Mo(N-N)(X)(\eta^3-C_3H_5)(CO)_2]$ complexes.^{19b} Attempted crystallization for the purpose of clarifying the disposition of the allyl group has so far been frustrating. Yet it is common to most known $[Mo(L-L)(X)(\eta^3\text{-allyl})(CO)_2]$ compounds that the allyl group and the two CO ligands define one face of the octahedron with the open face of the allyl pointing toward the carbonyls.^{9e,10,19,20}

In an analogous manner, the group 7 complexes **6** and **7** were also prepared in high yields as red crystalline solids by reacting **1** with $MX(CO)_5$ (M = Mn, Re; X = Br, Cl). Both compounds show three characteristic $\nu(CO)$ bands (2018 , 1917 , 1897 cm^{-1} for **6a**; 2013 , 1917 , 1877 cm^{-1} for **7a**) and three ^{13}C NMR signals in the carbonyl region (222.8 , 224.7 , 225.4 ppm for **6a**; 192.6 , 198.2 , 199.3 ppm for **7a**). Again the failure in obtaining single crystals from these complexes precluded us from locating the position of the halide ligand.

The cationic Pd(II) complexes (**8a,c**) were obtained as dark red crystals from the reaction of **1** with $[Pd(\eta^3-C_3H_5)Cl]_2$ followed by treatment with $AgBF_4$. Analytical and spectroscopic including HRMS data are fully consistent with the formulation of $[Pd(\eta^2-N,O)(\eta^3-C_3H_5)]^+BF_4^-$. A definitive evidence for the η^2-N,O chelation comes from the X-ray crystal structure of **8a** shown in Figure 2. A summary of crystallographic data and selected bond lengths and angles are listed in Tables 1 and 2, respectively. The geometry around palladium adopts a slightly distorted square plane, and the fused heterocyclic ring comprising the Pd-metallacycle and the ferrocenediylazaphosphinine ring forms an almost coplanar structure, as observed with **3a**. The Pd–O bond of $2.082(9)\text{ \AA}$ is slightly shorter than the Pd–N bond ($2.137(8)\text{ \AA}$) and also shorter than those found for the carbonyl group of a *P,O* chelate coordinated to a Pd

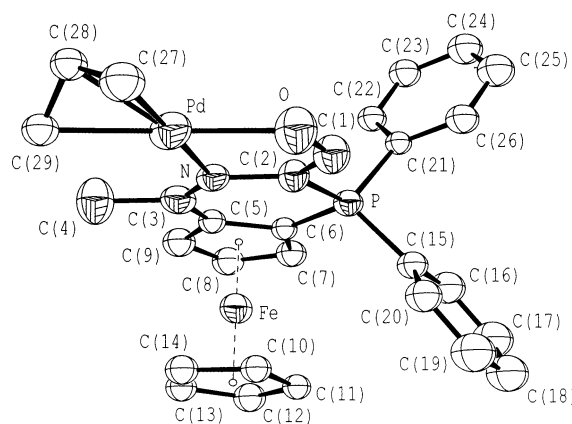


Figure 2. Crystal structure of **8a**. Thermal ellipsoids are drawn at 50% probability.

Table 3. Allylic Alkylation as a Function of Metal, Ligand, and Allyl Substrate^a

$ \begin{array}{c} \text{R}-\text{CH}=\text{CH}-\text{CH}_2\text{OAc} \xrightarrow[\text{THF or Dioxane}]{\text{Nu, [cat]}} \text{R}-\text{CH}=\text{CH}-\text{CH}_2\text{Nu} + \text{R}-\text{CH}=\text{CH}-\text{Nu} \\ \text{(9)} \qquad \qquad \qquad \text{(10)} \qquad \qquad \qquad \text{(11)} \end{array} $						
entry	catalyst	R	conditions		yield (%) ^b	ratio ^c 10:11
1	Mo(1a)(CO) ₄ , 2a	Pr	24	80	33	100:0
2	Mo(1a)(CO) ₄ , 2a	Ph	24	80	0	
3	Mo(1a)(CO) ₂ (π -C ₃ H ₅)(I), 4a	Pr	5	80	90	100:0
4	Mo(1b)(CO) ₂ (π -C ₃ H ₅)(I), 4b	Pr	24	80	66	100:0
5	Mo(1c)(CO) ₂ (π -C ₃ H ₅)(I), 4c	Pr	24	80	72	100:0
6	Mo(1a)(CO) ₂ (π -C ₃ H ₅)(I), 4a	Ph	24	80	0	
7	W(1a)(CO) ₄ , 3a	Pr	24	80	12	100:0
8	W(1a)(CO) ₄ , 3a	Ph	24	80	0	
9	W(1a)(CO) ₂ (π -C ₃ H ₅)(I), 5a	Pr	24	80	23	100:0
10	W(1a)(CO) ₂ (π -C ₃ H ₅)(I), 5a	Ph	24	80	0	
11	[Pd(1a)(π -C ₃ H ₅)]BF ₄ , 8a	Pr	5	RT	90	100:0
12	[Pd(1c)(π -C ₃ H ₅)]BF ₄ , 8c	Pr	24	70	90	100:0
13	[Pd(1a)(π -C ₃ H ₅)]BF ₄ , 8a	Ph	24	70	93	93:7
14	[Pd(1c)(π -C ₃ H ₅)]BF ₄ , 8c	Ph	24	70	88	92:8

^a Detailed procedure provided in Experimental Section: Nu = dimethyl malonate. ^b Isolated yield. ^c Determined by GC.

center.^{11,12} The steric repulsion between the allyl ligand and the methyl group at C(3) may be a contributing factor in lengthening the Pd–N bond distance. One of the most striking differences in the nature of chelation between **1** and most *P,O* chelates lies in the fact that the former, in contrast to the latter, shows no sign of hemilabile properties, as confirmed by their NMR (1H and ^{31}P) spectra. The room-temperature ^{31}P NMR spectrum of **8a**, for example, reveals only a sharp singlet at δ 4.80. The same NMR spectra allow us to confirm the static nature of the allyl group as well as the their presence.²¹ Yet, the three bond distances of Pd–C(27), Pd–C(28), and Pd–C(29) could not be determined without ambiguity due to the disorder of the allyl group at palladium. The C(1)–C(2) distance ($1.35(2)\text{ \AA}$) also carries a partial multiple-bond character.

Catalytic Allylic Alkylation. Table 3 shows the results on the catalytic allylic alkylation of unsymmetrically 1,3-disubstituted allyl derivatives as a function of metal, ligand, and allyl substrate. The most characteristic feature of the table is that all reactions involving hexenyl acetate (**9a**, $R = \text{Pr}$) exhibit a perfect regiocon-

(17) Sjögren, M. P. T.; Frisell, H.; Åkermark, B.; Norrby, P. O.; Eriksson, L.; Vitagliano, A. *Organometallics* **1997**, *16*, 942.

(18) Trost, B. M.; Lautens, M. *J. Am. Chem. Soc.* **1982**, *104*, 5543.

(19) (a) Pérez, J.; Riera, L.; Riera, V.; García-Granda, S.; García-Rodríguez, E. *J. Am. Chem. Soc.* **2001**, *123*, 7469. (b) Pérez, J.; Riera, L.; Riera, V.; García-Granda, S.; García-Rodríguez, E. *Organometallics* **2002**, *21*, 1622.

(20) Curtis, M. D.; Eisenstein, O. *Organometallics* **1984**, *3*, 887.

(21) Åkermark, B.; Krakenberger, B.; Hansson, S.; Vitagliano, A. *Organometallics* **1987**, *6*, 620.

trol in favor of a linear achiral isomer (**10a**) in high yields regardless of the metal or the ligand employed (entries 1, 3–5, 7, and 11–12). In particular, it is noteworthy to observe such a complete reversal of regioselectivity with our Mo- and W-based catalysts (**2–5**). As mentioned earlier, these results are quite contrary to those found with other Mo- and W-complexes incorporating such ligands as phosphinooxazolines or bis(2-pyridinecarboxamide)cyclohexane derivatives.⁹ Furthermore, the perfect regioselectivity as well as the high reactivity accomplished by catalysts **2–5** may well deserve comparison with those attainable by related Mo- and W-based catalysts. For instance, Mo(0) and Mo(II) complexes of the types Mo(N–N)(CO)₄ and [M(N–N)(π -allyl)(OTf)(CO)₂], where N–N represents various phenanthroline ligands, have been reported to exhibit much lower degrees of reactivity and regioselectivity for the same reaction, consequently giving rise to a distribution of various products.¹⁷ Of three types of catalysts we have employed, M(η^2 -N,O)(CO)₄ (**2** and **3**), [M(η^2 -N,O)(η^3 -C₃H₅)(I)(CO)₂] (**4** and **5**), and [Pd(η^2 -N,O)(η^3 -C₃H₅)]BF₄ (**8**), the first type has proved the least effective in that the reaction requires longer reaction time as well as higher reaction temperature only to give the lowest overall yields (<33%) (entries 1 and 7). When the comparison is made between molybdenum and tungsten, the former works more efficiently (entries 1 vs 7 and 3 vs 9). The structural variation in the ligand from **1a** to **1c** has little effect on the regioselectivity of the reaction (entries 3–5 and 11–12). An additionally striking feature of Table 3 is that for an unknown reason, Mo- and W-based catalysts (**2–5**) are totally ineffective for the conversion of cinnamyl acetate (**9b**, R = Ph) toward the formation of either **10b** or **11b** (entries 2, 6, 8, and 10). This was evidenced by near quantitative recovery of the starting compound in the form of cinnamyl alcohol (PhCH=CHCH₂OH) that might have been formed as a result of simple hydrolysis of the reactant acetate under the basic workup conditions. On the other hand, the Pd-catalysts (**8**), the most efficient of all, catalyze the allylation of both hexenyl acetate (**9a**) and cinnamyl acetate (**9b**) alike, producing the linear isomer (**10**) with near perfect regioselectivity (entries 11–14).

Although much has yet to be known concerning the origin of such unique regioselectivity demonstrated by our catalytic systems, it may be safe to state that the unsymmetric bonding nature of the ligand (**1**) should exhibit an electronic and/or steric bias for the disposition of the unsymmetrically substituted allyl derivatives in the coordination sphere and the subsequent attack of the nucleophile as well. Finally, according to the results in Table 3, our catalysts (**2–5**, **8**) are not suitable as a probe for enantioselectivity of unsymmetric 1,3-disubstituted allyl substrates. However, they bear some synthetic advantages in that they negate the preparation and employment of (C₇H₈)M(CO)₃ or (EtCN)₃M(CO)₃ as the precatalyst, which requires laborious preparative work and careful handling.

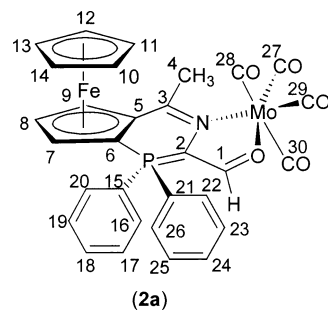
In this regard the way may be open for these complexes in their enantiomerically pure forms to be employed in the asymmetric allylic alkylation of symmetrically 1,3-disubstituted allyl derivatives such as 1,3-

diphenyl-2-propenyl acetate (**12**). Quite disappointingly, however, all of Mo- and W-based complexes (**2–5**) exhibit near zero catalytic activity under the standard set of reaction conditions, as were the cases with the reaction of cinnamyl acetate (cf. entries 2, 6, 8, 10, Table 3). Only Pd-complexes (**8a,c**) catalyze the reaction to give **13** with high chemical yields and a certain degree of enantiomeric excess reaching 50% ee. Studies on fine-tuning of the catalysts to improve their enantioselection are currently underway and will be the subject of our future communication.

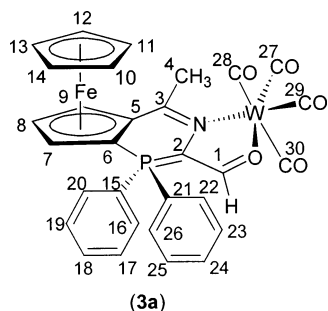
Experimental Section

General Remarks. All reactions were carried out under an atmosphere of nitrogen using standard Schlenk techniques. Solvents were dried using standard procedures. The ¹H and ¹³C NMR experiments were performed on a Bruker Advance 400 or 500 spectrometer. The ³¹P NMR spectra were recorded on a Varian Unity Inova 300 WB spectrometer. Chemical shifts are given as δ values with reference to tetramethylsilane (TMS) as internal standard. Coupling constants are in Hz. GC–mass spectra were obtained by using a Micromass QUATRO II GC8000 series model with electron energy of 20 or 70 eV. IR spectra were run on a Mattson FT-IR Galaxy 6030E spectrophotometer. All commercial reagents were purchased from Aldrich and used as received. 1,2-Ferrocenediylazaphosphinines (**1a–c**) were prepared according to the methods described earlier by us.¹

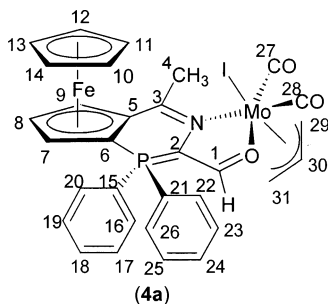
Synthesis of 2a. A 50 mL, two-necked round-bottom flask equipped with a condenser was charged with **1a** (0.50 g, 1.10 mmol) and Mo(CO)₆ (0.33 g, 1.23 mmol) in a mixture of THF (10 mL) and toluene (25 mL). The mixture was stirred at 90 °C for 3 h, during which time the solution turned deep red. Chromatographic separation on silica gel with a mixture of MeOH and diethyl ether (9:1) as an eluent followed by removal of solvents gave red solids. Recrystallization from CH₂Cl₂/diethyl ether yielded 0.55 g of **2a** (76%) in two crops as red crystals. ³¹P NMR (121 MHz, CDCl₃, H₃PO₄): δ 4.99 (s). ¹H NMR (400 MHz, CDCl₃): δ 2.78 (s, H4), 3.91 (s, H10–H14), 4.78 (m, H7), 4.88 (m, H8), 5.02 (m, H9), 7.22–7.27 (m, H22/H26), 7.34–7.41 (m, H23/H25), 7.49–7.60 (m, H24), 7.67–7.70 (m, H16/H20), 7.70–7.78 (m, H18), 7.84–7.88 (m, H17/H19), 8.16 (d, *J* = 1.0, H1). ¹³C NMR (100.6 MHz, CDCl₃): δ 28.4 (s, C4), 60.4 (d, *J* = 101.6, C6), 71.9 (d, *J* = 6.7, C9), 72.3 (d, *J* = 8.2, C7), 72.4 (s, C10–C14), 76.3 (d, *J* = 11.6, C8), 81.2 (d, *J* = 7.0, C5), 94.2 (d, *J* = 101.6, C2), 125.4 (d, *J* = 94.1, C15), 128.2 (d, *J* = 89.1, C21), 130.1 (d, *J* = 12.6, C22/C26), 130.3 (d, *J* = 13.2, C17/C19), 133.6 (d, *J* = 10.9, C16/C20), 133.7 (d, *J* = 11.0, C23/C25), 133.9 (d, *J* = 2.8, C24), 134.9 (d, *J* = 3.3, C18), 154.8 (d, *J* = 7.7, C3), 179.9 (d, *J* = 33.0, C1), 205.6 (s), 206.2 (s), 224.3 (s), 225.2 (s) (C27–C30). IR ν (CO): 1882 (vs), 1855 (vs), 1803 (vs) cm⁻¹. HRMS (EI, *m/z*): calcd for C₃₀H₂₂NPO₅FeMo 661.9717 (M⁺), found 632.9708 (M⁺ – CO). Anal. Calcd for C₃₀H₂₂NPO₅FeMo: C, 54.66; H, 4.36; N, 2.12. Found: C, 54.35; H, 4.19; N, 1.64.



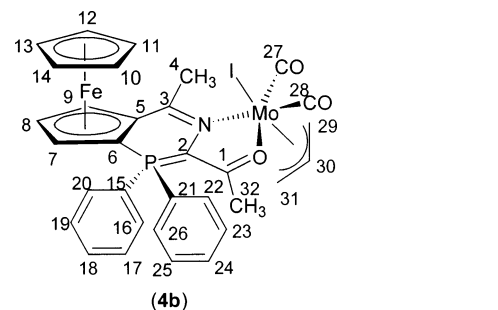
Synthesis of 3a. This compound was prepared in the same manner as described above replacing $\text{Mo}(\text{CO})_6$ with $\text{W}(\text{CO})_6$ as a reagent. Yield: 0.76 g, 92%. Red single crystals suitable for X-ray structural determination were grown by slow diffusion of diethyl ether into a solution of **3a** in CH_2Cl_2 . ^{31}P NMR (121 MHz, CDCl_3 , H_3PO_4): δ 5.72 (s). ^1H NMR (400 MHz, CDCl_3): δ 2.83 (s, H4), 3.94 (s, H10–H14), 4.80 (m, H7), 4.91 (m, H8), 5.04 (m, H9), 7.25–7.29 (m, H22/H26), 7.40–7.43 (m, H23/H25), 7.52–7.55 (m, H24), 7.68–7.72 (m, H16/H20), 7.76–7.80 (m, H18), 7.84–7.89 (m, H17/H19), 8.26 (d, J = 2.0, H1). ^{13}C NMR (100.6 MHz, CDCl_3): δ 29.4 (s, C4), 60.3 (d, J = 102.8, C6), 72.4 (d, J = 6.3, C9), 72.5 (d, J = 7.2, C7), 72.6 (s, C10–C14), 76.6 (d, J = 12.1, C8), 81.1 (d, J = 7.6, C5), 97.4 (d, J = 104.4, C2), 124.9 (d, J = 94.5, C15), 127.7 (d, J = 89.6, C21), 130.2 (d, J = 13.2, C22/C26), 130.4 (d, J = 13.2, C17/C19), 132.6 (d, J = 11.6, C16/C20), 133.6 (d, J = 10.9, C23/C25), 134.2 (d, J = 2.8, C24), 135.2 (d, J = 2.8, C18), 156.7 (d, J = 7.6, C3), 181.3 (d, J = 31.5, C1), 204.0 (s), 204.5 (s), 216.5 (s), 217.3 (s) (C27–C30). IR $\nu(\text{CO})$: 1868 (vs), 1845 (vs), 1800 (vs) cm^{-1} . HRMS (EI, m/z): calcd for $\text{C}_{30}\text{H}_{22}\text{NPO}_5\text{FeW}$ 747.0095 (M^+), found 747.0115. Anal. Calcd for $\text{C}_{30}\text{H}_{22}\text{NPO}_5\text{FeW}$: C, 48.19; H, 2.95; N, 1.87. Found: C, 48.32; H, 2.69; N, 1.74.



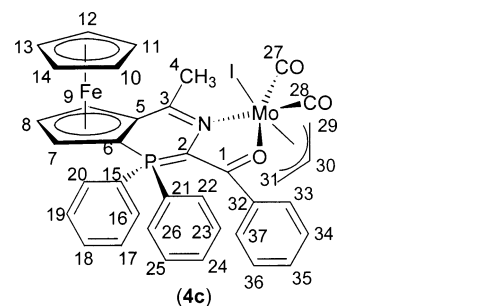
Synthesis of 4a. To a solution of **2a** (0.81 g, 1.2 mmol) in THF (20 mL) was added a 2 molar excess of allyl iodide (0.20 mL), and the reaction mixture was stirred under reflux for 2 h. The solvent was removed under vacuum, and the oily residue was chromatographed on silica gel (eluent: diethyl ether/MeOH, 8:2) to give dark red solids after usual workups. Yield: 47%. ^{31}P NMR (202.5 MHz, CD_2Cl_2 , H_3PO_4): δ 4.48 (s). ^1H NMR (500 MHz, CD_2Cl_2): δ 2.93 (s, H4), 3.00–3.07 (m, *anti*-H29/H31), 4.47–4.07 (m, *syn*-H29/H31), 4.01 (s, H10–H14), 4.71 (s, H7), 4.78 (br, H8), 4.89 (s, H9), 5.01 (br, H30), 7.24–7.28 (m, H22/H26), 7.43–7.47 (m, H23/H25), 7.53–7.56 (m, H24), 7.63–7.65 (m, H16/H20), 7.70–7.73 (m, H18), 7.89–7.92 (m, H17/H19). ^{13}C NMR (125.8 MHz, CD_2Cl_2): δ 25.0 (s, C4), 61.0 (br, C6), 71.9 (s, C10–C14), 71.7 (s, C7), 72.1 (br, C9), 74.8 (s)/75.3 (s) (C29/C31), 76.9 (br, C8), 79.2 (br, C5), 84.9 (d, J_P = 46.7, C2), 117.8 (s, C30), 123.9 (br, C15), 128.4 (br, C21), 129.0 (d, J_P = 12.7, C22/C26), 129.8 (br, C17/C19), 131.8 (br, C16/C20), 133.0 (d, J_P = 11.6, C23/C25), 134.4 (br, C18), 154.8 (br, C3), 172.8 (d, J_P = 29.6, C1), 227.4 (s)/227.9 (s) (C27/C28). IR $\nu(\text{CO})$: 1923 (vs), 1831 (vs) cm^{-1} . HRMS (EI, m/z): calcd for $\text{C}_{31}\text{H}_{27}\text{NPO}_3\text{IMoFe}$ 772.9177, found 772.9177. Anal. Calcd for $\text{C}_{31}\text{H}_{27}\text{NPO}_3\text{IMoFe}$: C, 48.30; H, 3.50; N, 1.80. Found: C, 48.47; H, 3.77; N, 1.62.



Synthesis of 4b. Yield: 50%. ^{31}P NMR (202.5 MHz, CD_2Cl_2 , H_3PO_4): δ 2.95 (s). ^1H NMR (500 MHz, CD_2Cl_2): δ 1.43 (d, J = 8.0, H32), 1.75 (s, H4), 3.37–3.51 (m, *anti*-H29/H31), 3.91 (s, H10–H14), 4.16 (s, H7), 4.34–4.52 (m, *syn*-H29/H31), 4.63 (br, H8), 4.82 (s, H9), 5.10 (m, H30), 7.38–7.43 (m, H22–H26), 7.49 (m, H23/H25), 7.54–7.58 (m, H24), 7.66 (m, H16/H20), 7.90 (m, H18), 8.25 (m, H17/H19). ^{13}C NMR (125.8 MHz, CD_2Cl_2): δ 26.0 (s, C32), 30.2 (s, C4), 61.5 (d, J = 105.0, C6), 70.8 (d, J = 83.4, C9), 71.9 (d, J = 31.0, C7), 71.8 (s, C10–C14), 75.5 (d, J = 12.2, C8), 80.6 (s, C5), 128.1 (br, C15), 128.3 (br, C21), 129.2 (d, J = 13.9, C22/C26), 129.5 (d, J = 13.7, C17/C19), 131.5 (br, C16/C20), 132.9 (br, C23/C25), 133.5 (s, C18), 133.7 (s, C24), 187.0 (d, J = 29.1, C1), 228.0 (s)/228.4 (s) (C27/C28). IR $\nu(\text{CO})$: 1927 (vs), 1833 (vs) cm^{-1} . HRMS (EI, m/z): calcd for $\text{C}_{32}\text{H}_{29}\text{NPO}_3\text{IMoFe}$ 786.9333, found 730.9453 ($\text{M}^+ - 2\text{CO}$). Anal. Calcd for $\text{C}_{32}\text{H}_{29}\text{NPO}_3\text{IMoFe}$: C, 48.95; H, 3.72; N, 1.78. Found: C, 48.95; H, 3.35; N, 2.01.

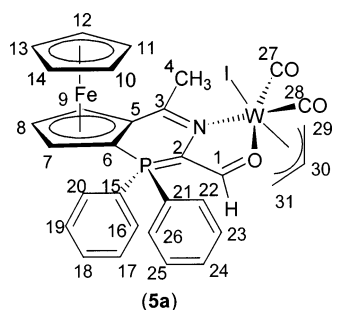


Synthesis of 4c. Yield: 61%. ^{31}P NMR (202.5 MHz, CD_2Cl_2 , H_3PO_4): δ 2.89 (s). ^1H NMR (500 MHz, CD_2Cl_2): δ 2.77 (s, H4), 3.20 (m, *anti*-H29/H31), 3.93 (s, H10–H14), 4.50 (s, H7), 4.54 (m, *syn*-H29/H31), 4.78 (m, H8), 5.04 (m, H30), 5.09 (s, H9), 6.62 (m, H33/H37), 6.74 (m, H34/H36), 6.87 (m, H35), 7.15 (m, H24), 7.22 (m, H22/H26), 7.43 (m, H23/H25), 7.64 (m, H16/H20), 7.76 (m, H17/H19), 7.93 (m, H18). ^{13}C NMR (125 MHz, CDCl_3) for selected nuclei: δ 29.1 (s, C4), 72.1 (s, C10–C14), 188.5 (d, J = 29.1, C1), 212.3 (s) and 226.6 (s) (C27/C28), 109.9 (s, C30). HRMS (EI, m/z): calcd for $\text{C}_{37}\text{H}_{31}\text{NPO}_3\text{IMoFe}$ 848.9490, found 792.9589 ($\text{M}^+ - 2\text{CO}$). Anal. Calcd for $\text{C}_{37}\text{H}_{31}\text{NPO}_3\text{IMoFe}$: C, 52.30; H, 3.65; N, 1.65. Found: C, 52.85; H, 3.95; N, 1.97.

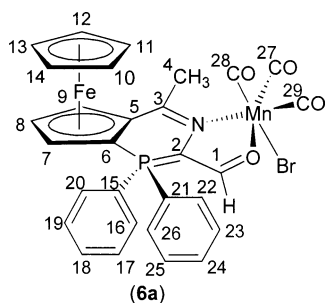


Synthesis of 5a. The title compound was prepared in the same manner as described for the preparation of **4a** by replacing **2a** with **3a**. Yield: 85%. ^{31}P NMR (121 MHz, CDCl_3 , H_3PO_4): δ 4.35 (s). ^1H NMR (500 MHz, CD_2Cl_2): δ 2.76 (s, H4), 2.98 (m, *anti*-H29/H31), 4.19 (s, H10–H14), 4.45–4.30 (m, *syn*-H29/H31), 4.90 (s, H7), 5.03 (m, H8), 5.10 (s, H9), 7.95 (s, H1), 8.14–7.51 (m, H15–H26). ^{13}C NMR (125.8 MHz, CDCl_3): δ 30.2 (s, C4), 69.9 (br, C6), 70.5 (br, C9), 71.6 (br, C7), 72.6 (br, C8), 72.9 (s, C10–C14), 128.0 (br, C15), 128.2 (br, C21), 129.6 (br, C22/C26), 129.9 (d, J = 13.3, C17/C19), 131.5 (br, C23/C25), 132.1 (d, J = 0.8, C16/C20), 133.3 (s, C24), 134.8 (s, C18), 158.3 (br, C3), 177.7 (br, C1), 217.3 (s)/229.3 (s) (C27/C28). IR $\nu(\text{CO})$: 1912 (s), 1814 (s) cm^{-1} . HRMS (EI,

m/z): calcd for $C_{31}H_{27}NPO_3IWFe$ 858.9632, found 858.9622. Anal. Calcd for $C_{31}H_{27}NPO_3IWFe$: C, 43.31; H, 3.14; N, 1.63. Found: C, 43.29; H, 3.68; N, 1.42.

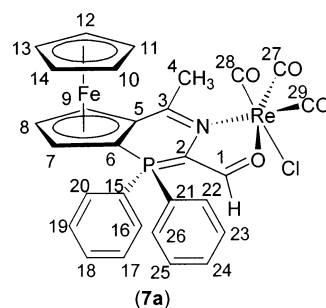


Synthesis of 6a. A solution of **1a** (0.50 g, 1.10 mmol) and $Mn(CO)_5Br$ (0.31 g, 1.10 mmol) in THF (10 mL) in a Schlenk tube equipped with a condenser was heated under reflux for 5 h. The solvent was removed under vacuum, and the remaining red solid was chromatographed on silica gel (eluent: diethyl ether/MeOH, 1:9). Recrystallization from CH_2Cl_2 /hexanes yielded the product as red crystals. Yield: 85%. ^{31}P NMR (121 MHz, $CDCl_3$, H_3PO_4): δ 3.56 (s). 1H NMR (400 MHz, $CDCl_3$): δ 2.87 (s, H4), 3.96 (s, H10–H14), 4.78 (m, H7), 4.89 (m, H8), 5.02 (m, H9), 7.24 (br, H22/H26), 7.40 (br, H23/H25), 7.52 (br, H24), 7.65 (br, H16/H20), 7.70 (br, H18), 8.03 (br, H17/H19), 8.20 (d, $J = 2.0$, H1). ^{13}C NMR (100.6 MHz, $CDCl_3$): δ 27.5 (s, C4), 69.0 (d, $J = 103.3$, C6), 72.4 (d, $J = 6.3$, C9), 72.5 (d, $J = 7.2$, C7), 72.6 (s, C10–C14), 76.7 (d, $J = 12.1$, C8), 81.3 (d, $J = 7.7$, C5), 95.3 (d, $J = 106.0$, C2), 124.9 (d, $J = 94.5$, C15), 127.7 (d, $J = 89.6$, C21), 130.2 (d, $J = 13.2$, C22/C26), 130.4 (d, $J = 13.2$, C17/C19), 132.6 (d, $J = 11.6$, C16/C20), 133.6 (d, $J = 10.9$, C23/C25), 134.2 (d, $J = 2.8$, C24), 135.2 (d, $J = 2.8$, C18), 154.4 (d, $J = 7.6$, C3), 180.9 (d, $J = 30.2$, C1), 222.8 (s, 224.7 (s), 225.4 (s) (C27–C29). IR $\nu(CO)$: 2018 (vs), 1917 (vs), 1897 (vs) cm^{-1} . HRMS (EI, m/z): calcd for $C_{29}H_{22}NPO_4BrFeMn$ 670.1501 (M^+), found 584.8850 ($M^+ - 3CO$). Anal. Calcd for $C_{29}H_{22}NPO_4BrFeMn$: C, 51.97; H, 3.31; N, 2.09. Found: C, 52.08; H, 3.36; N, 1.99.

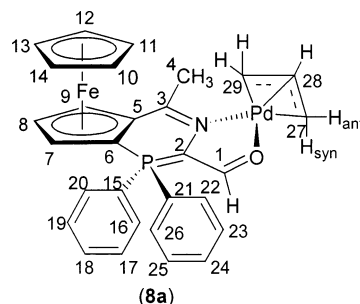


Synthesis of 7a. Following the procedure for the synthesis of **6a** except for the replacement of $MnBr(CO)_5$ with $ReCl(CO)_5$, an orange solid was isolated in 95%. 1H NMR (400 MHz, $CDCl_3$): δ 2.84 (s, H4), 4.00 (s, H10–H14), 4.83 (m, H7), 4.95 (m, H8), 5.08 (m, H9), 7.26–7.30 (m, H22/H26), 7.41–7.44 (m, H23/H25), 7.54–7.57 (m, H24), 7.69–7.71 (br, H16/H20), 7.74–7.77 (m, H18), 8.07–8.11 (m, H17/H19), 8.17 (d, H1, $J = 2.0$). ^{13}C NMR (100.6 MHz, $CDCl_3$): δ 29.3 (s, C4), 181.1 (d, $J = 31.3$, C1), 59.3 (d, $J = 102.7$, C6), 73.1 (d, $J = 5.0$, C9), 73.2 (d, $J = 3.8$, C7), 73.5 (s, C10–C14), 77.1 (d, $J = 12.2$, C8), 80.2 (d, $J = 7.6$, C5), 98.5 (d, $J = 107.7$, C2), 125.7 (d, $J = 95.1$, C15), 128.0 (d, $J = 90.7$, C21), 130.2 (d, $J = 25.7$, C22/C26), 130.3 (d, $J = 10.2$, C17/C19), 132.6 (d, $J = 11.4$, C16/C20), 134.1 (d, $J = 12.0$, C23/C25), 134.2 (d, $J = 2.8$, C24), 135.2 (d, $J = 3.3$, C18), 157.8 (d, $J = 8.7$, C3), 192.6 (s), 198.2 (s), 199.3 (s) (C27–C29). IR $\nu(CO)$: 2013 (vs), 1917 (vs), 1877 (vs) cm^{-1} . HRMS (EI, m/z): calcd for $C_{29}H_{22}NPO_4ClFeRe$

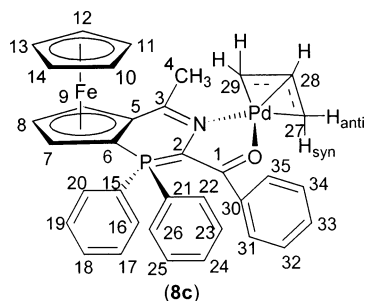
756.9882 (M^+), found 756.9873. Anal. Calcd for $C_{29}H_{22}NPO_4ClFeRe$: C, 45.97; H, 2.91; N, 1.85. Found: C, 46.02; H, 3.25; N, 1.97.



Synthesis of 8a. $[Pd(\eta^3-C_3H_5)Cl]_2$ (0.12 g, 0.33 mmol) and **1a** (0.30 g, 0.66 mmol) were dissolved in CH_2Cl_2 (5 mL) in a Schlenk tube. The mixture was stirred at room temperature for 30 min, after which $AgBF_4$ (0.13 g, 0.66 mmol) was added. Any solid impurities were removed by filtration, and the volume of the filtrate was reduced to about 2 mL. Slow diffusion of diethyl ether into this solution at room temperature produced red crystals. A single crystal obtained in this way was used for the X-ray analysis. Yield: 0.39 g, 86%. ^{31}P NMR (202 MHz, $CDCl_3$, H_3PO_4): δ 4.80 (s). 1H NMR (500 MHz, CD_2Cl_2): δ 2.58 (s, H4), 2.99–3.30 (m, *anti*-H27/H29), 3.94 (s, H10–H14), 4.30–4.06 (m, *syn*-H27/H29), 4.96 (br, 7H), 5.08 (br, H8), 5.19 (br, H9), 5.58 (m, H28), 7.25 (m, H22/H26), 7.43 (m, H23/H25), 7.56 (m, H24), 7.75 (m, H16/H20), 7.80 (m, H18), 7.90 (m, H17/H19), 8.10 (br, H1). ^{13}C NMR (100.6, CD_2Cl_2): δ 29.9 (s, C4), 57.5 (br, C7), 60.0 (d, $J = 103.7$, C6), 63.3 (br, C9), 72.9 (s, C10–C14), 74.0 (s, C27/C29), 77.8 (d, $J = 12.0$, C8), 79.5 (br, C5), 96.5 (d, $J = 107.7$, C2), 114.4 (s, C28), 127.6 (d, $J = 89.5$, C15/C21), 130.3 (d, $J = 13.0$, C22/C26), 130.6 (d, $J = 13.7$, C17/C19), 132.4 (br, C16/C20), 133.6 (br, C23/C25), 134.3 (br, C24), 135.5 (br, C18), 158.7 (d, $J = 6.7$, C3), 180.0 (d, $J = 31.8$, C1). HRMS (EI, m/z): calcd for $C_{29}H_{27}NPOFePd$ 598.0214 (M^+), found 598.0212. Anal. Calcd for $C_{29}H_{27}NPOBF_4FePd$: C, 50.81; H, 3.97; N, 2.04. Found: C, 50.59; H, 4.06; N, 1.91.



Synthesis of 8c. ^{31}P NMR (202 MHz, $CDCl_3$, H_3PO_4): δ 4.48 (s). 1H NMR (500 MHz, CD_2Cl_2): δ 2.78 (s, H4), 2.99 (m, *anti*-H27/H29), 3.86 (s, H10–H14), 4.08 (m, *syn*-H27/H29), 4.82 (s, H7), 5.01 (m, H8), 5.25 (s, H9), 5.62 (m, H28), 6.85–6.69 (m, 5H, H30–H35), 7.98–7.04 (m, 10H, H15–H26). ^{13}C NMR (125 MHz, $CDCl_3$): δ 30.5 (s, C4), 62.8 (d, $J = 101.6$, C6), 71.5 (s, C27/C29), 73.3 (d, $J = 6.5$, C7), 74.3 (d, $J = 8.2$, C9), 77.9 (br, C8), 94.6 (d, $J = 101.6$, C2), 114.0 (s, C28), 125.7 (d, $J = 170.0$, C15), 125.7 (d, $J = 16.4$, C30), 128.7 (d, $J = 129.5$, C21), 129.1 (s, C32/C34), 129.5 (d, $J = 20.9$, C22/C26), 130.0 (d, $J = 13.2$, C17/C19), 131.1 (d, $J = 68.1$, C31/C35), 131.8 (s, C33), 133.1 (d, $J = 11.1$, C23/C25), 133.0 (d, $J = 7.3$, C16/C20), 134.5 (s, C24), 137.3 (s, C18), 160.4 (br, C3), 189.5 (d, $J = 30.3$, C1). HRMS (EI, m/z): calcd for $C_{35}H_{31}NPOFePd$ 674.0527 (M^+), found 674.0526. Anal. Calcd for $C_{35}H_{31}NPOF_4FePd$: C, 55.19; H, 4.10; N, 1.84. Found: C, 55.63; H, 4.37; N, 1.31.



Typical Procedure for Allylic Alkylation. To a solution of dimethylsodium malonate (prepared from dimethyl malonate (40.0 mg, 0.30 mmol) and NaH (5.3 mg, 0.22 mmol) in 2,4-dioxane or THF (1.0 mL) at RT) and allyl substrate (0.17 mmol) was added catalyst (0.025 mmol for Mo- and W-catalysis; 0.017 mmol for Pd-catalysis). The mixture was stirred at 80 °C (RT in the case of Pd-catalysis) until the reaction was complete (as evidenced by TLC), then diluted with ether (2 mL), and washed successively with 5% aqueous NaHCO₃ and water. The organic phase was dried with MgSO₄, and the solvent was evaporated under reduced pressure. The oily residue was passed through a short silica gel column to remove catalyst using a 9:1 hexane–ethyl acetate mixture as an eluent. The diastereomeric excess (% de) was determined by GC equipped with a CBP-10 on a Shimadzu GC-17A.

Typical Procedure for Asymmetric Allylic Alkylation. A mixture of chiral ligand (0.02 mmol) and [Pd(η^3 -C₃H₅)Cl]₂ (0.02 mmol) in a dry solvent (2 mL) was stirred at RT in a Schlenk tube. To this Pd-catalyst generated *in situ* was added a solution of 1,3-diphenyl-2-propenyl acetate (**12**) (0.13 g, 0.50 mmol) in the same solvent (2 mL), followed by the addition of dimethyl malonate (0.17 mL, 1.50 mmol), KOAc (0.001 g, 0.01 mmol), and *N,O*-bis(trimethylsilyl)acetamide (0.37 mL, 1.50 mmol). The reaction mixture was heated under reflux for 24 h. After cooling to room temperature, the reaction mixture was diluted with diethyl ether (10 mL) and water, and the organic layer was washed with brine and dried over MgSO₄. After evaporation of solvent *in vacuo*, the residue was purified by column chromatography on silica gel (eluent, hexane–ethyl acetate, 9:1). The enantioselectivity was determined by HPLC analysis with a chiral column (Chiralcel OD-H; 25 cm \times 0.46 cm; hexane/*i*-PrOH, 99:1; flow rate, 0.6 mL/min; *t_R*, 21.680; *t_S*, 23.301 min) and ¹H NMR analysis with chiral shift reagent Eu(hfc)₃ (one of two methyl ester groups that appears at 3.70 was split into two peaks, for example, at 3.78 (*R*) and 3.74 (*S*) when 0.5 equiv of the chiral shift reagent was added).²²

Dimethyl 2-[(*E*)-Hex-2-enyl]propanedioate (10a**).** This was obtained as the product from the reaction of (*E*)-1-acetoxy-2-hexene with dimethylsodium malonate. GC (CBP-10) conditions for diastereomeric separation: *t_R*, 15.4 min; oven temp, 100 °C; injection temp, 220 °C, initial time, 2 min; final temp, 200 °C; rate, 5 °C/min; detection temp, 250 °C; column pressure, 100 kPa. IR (KBr): 2958 (s), 2930 (m), 2850 (m), 1737 (s), 1457 (m), 1379 (m), 1274 (s), 1146 (m), 973 (m), 745 (w) cm⁻¹. ¹H NMR (300 MHz, CDCl₃): δ 5.79 (m, 1H), 5.56 (m, 1H), 4.59 (d, *J* = 6.3, 2H), 3.75 (s, 6H), 3.40 (br, 1H), 2.02 (dq, *J* = 21.3, 6.9, 2H), 1.42 (sextet, *J* = 36.9, 2H), 0.90 (t, *J* = 14.7, 3H). ¹³C NMR (75 MHz, CDCl₃): δ 169.1, 137.1, 123.2,

52.5, 41.4, 34.3, 29.7, 22.0, 13.6. MS: *m/z* (%) 214 (1, M⁺), 182 (3), 165 (2), 132 (9), 119 (100), 101 (70), 83 (80), 67 (50), 55 (51).

Dimethyl 2-(1-Phenylprop-2-enyl)propanedioate (11a**).** GC (CBP-10) conditions for diastereomeric separation: *t_R*, 22.4 min; oven temp, 100 °C; injection temp, 220 °C, initial time, 2 min; final temp, 200 °C; rate, 5 °C/min; detection temp, 250 °C; column pressure, 100 kPa. IR (KBr): 3031 (w), 2954 (m), 1760 (s), 1740 (s), 1639 (w), 1602 (w), 1494 (w), 1435 (m), 1263 (m), 1198 (m), 1163 (m), 1027 (w), 765 (w) cm⁻¹. ¹H NMR (300 MHz, CDCl₃): δ 7.32–7.19 (m, 5H), 5.99 (ddd, *J* = 17.0, 10.2, 8.1, CH), 5.15–5.06 (m, 2H), 4.14–4.08 (m, CH), 3.87 (d, *J* = 11.0, CH), 3.74, 3.49 (2s, 6H). ¹³C NMR (75 MHz, CDCl₃): δ 168.2, 167.8, 139.9, 137.8, 128.7, 127.9, 127.1, 116.6, 57.4, 52.6, 52.4, 49.7. MS: *m/z* (%) 248 (2, M⁺), 217 (2), 189 (100), 156 (19), 129 (43), 117 (100), 91 (19).

Dimethyl 2-[(*E*)-3-Phenylprop-2-enyl]propanedioate (10b**).** GC (CBP-10) conditions for diastereomeric separation: *t_R*, 29.6 min; oven temp, 100 °C; injection temp, 220 °C, initial time, 2 min; final temp, 200 °C; rate, 5 °C/min; detection temp, 250 °C; column pressure, 100 kPa. *R_f* = 0.32 (hexane/EtOAc, 6:1). IR (KBr): 3448 (s), 2359 (w), 1734 (m), 1635 (s), 1435 (w), 1261 (w), 1153 (m), 966 (w), 749 (m) cm⁻¹. ¹H NMR (300 MHz, CDCl₃): δ 7.20–7.34 (m, 5 arom. CH), 6.48 (d, *J* = 15.6, CH), 6.16 (dt, *J* = 15.8, 7.2, CH), 3.74 (s, 2 OCH₃), 3.53 (t, *J* = 14.7, CHCO), 2.80 (dt, *J* = 15.9, 1.2, CH₂). ¹³C NMR (75 MHz, CDCl₃): δ 169.1 (C=O), 136.9 (arom. C), 132.8 (CH), 128.4 (CH), 127.3 (CH), 126.1 (CH), 125.3 (CH), 52.4, 51.6 (CH, Me), 32.2 (CH₂). MS: *m/z* (%) 248 (30, M⁺), 188 (38), 157 (20), 129 (100), 117 (61), 84 (19).

Dimethyl 2-(1,3-Diphenylprop-2-enyl)propanedioate (13**).** ¹H NMR (500 MHz, CDCl₃): δ 3.51 (s, OCH₃), 3.70 (s, OCH₃), 3.95 (d, *J* = 11, CHCO), 4.26 (dd, *J* = 9 and 11, PhCH), 6.33 (dd, *J* = 9 and 16, PhCH=CH), 6.47 (d, *J* = 16, PhCH=CH), 7.18–7.33 (m, Ph). ¹³C NMR (75 MHz, CDCl₃): δ 49.2 (CHPh), 52.5 (OCH₃), 52.6 (OCH₃), 57.6 (CHCO), 126.4/127.2 (PhCH=CH), 127.6/127.9/128.4/128.7/129.1/131.8/136.8/140.2 (Ph), 167.6/167.8 (C=O).

X-ray Structure Determination. Crystallographic data for **3a** and **8a** are collected in Tables 1 and 2. An ORTEP drawing showing the numbering scheme used in refinement is presented in Figures 1 and 2. Intensity data were collected at room temperature with a CAD4 diffractometer using monochromated Mo K α radiation (λ = 0.71073 Å). Lorentz and polarization reflections were applied and absorption corrections made with 3 Ψ scans. The structures were solved by direct methods and refined by full-matrix least-squares methods based on *F*² using SHELXS-97 and SHELXL-97.²³ Non-hydrogen atoms were refined anisotropically, and hydrogen atoms were included in calculated positions. Additional crystallographic data are available in the Supporting Information.

Acknowledgment. T.J.K. gratefully acknowledges KRF for financial support (Grant No.: PBRG 070-C00055) and KBSI for NMR and mass spectral measurements.

Supporting Information Available: Tables giving atomic coordinates, displacement parameters, and bond distances and angles for **3a** and **8a**. This material is available free of charge via the Internet at <http://pubs.acs.org>.

OM020929N

(22) (a) Ahn, K. H.; Cho, C.-W.; Park, J. W.; Lee, S. W. *Tetrahedron Asymmetry* **1997**, 8, 1179. (b) Chelucci, G.; Deriu, S.; Pinna, G. A.; Saba, A.; Valenti, R. *Tetrahedron Asymmetry* **1999**, 10, 3803. (c) You, S.-L.; Hou, X.-L.; Dai, L.-X.; Yu, Y.-H.; Xia, W. *J. Org. Chem.* **2002**, 67, 4684.

(23) Sheldrick, G. M. *SHELXS-86*; Universität Göttingen: 1986; *SHELXL-97*; Universität Göttingen: 1997.